energies

MDPI

Article

Dynamic Simulation and Thermoeconomic Analysis of a Trigeneration System in a Hospital Application

Francesco Calise, Francesco Liberato Cappiello *, Massimo Dentice d'Accadia, Luigi Libertini and Maria Vicidomini

Department of Industrial Engineering, University of Naples Federico II, 80125 Naples, Italy; frcalise@unina.it (F.C.); dentice@unina.it (M.D.d.); libertiniluigi@gmail.com (L.L.); maria.vicidomini@unina.it (M.V.)

* Correspondence: francescoliberato.cappiello@unina.it

Received: 1 June 2020; Accepted: 7 July 2020; Published: 10 July 2020

Abstract: Hospitals are very attractive for Combined Heat and Power (CHP) applications, due to their high and continuous demand for electric and thermal energy. However, both design and control strategies of CHP systems are usually based on an empiric and very simplified approach, and this may lead to non-optimal solutions. The paper presents a novel approach based on the dynamic simulation of a trigeneration system to be installed in a hospital located in Puglia (South Italy), with around 600 beds, aiming to investigate the energy and economic performance of the system, for a given control strategy (electric-load tracking). The system includes a natural gas fired reciprocating engine (with a rated power of 2.0 MW), a single-stage LiBr-H_2O absorption chiller (with a cooling capacity of around 770 kW), auxiliary gas-fired boilers and steam generators, electric chillers, cooling towers, heat exchangers, storage tanks and several additional components (pipes, valves, etc.). Suitable control strategies, including proportional–integral–derivative (PID) and ON/OFF controllers, were implemented to optimize the trigeneration performance. The model includes a detailed simulation of the main components of the system and a specific routine for evaluating the heating and cooling demand of the building, based on a 3-D model of the building envelope. All component models were validated against experimental data provided by the manufacturers. Energy and economic models were also included in the simulation tool, to calculate the thermoeconomic performance of the system. The results show an excellent economic performance of the trigeneration system, with a payback period equal to 1.5 years and a profitability index (ratio of the Net Present Value to the capital cost) equal to 3.88, also due to the significant contribution of the subsidies provided by the current Italian regulation for CHP systems (energy savings certificates).

Keywords: cogeneration; absorption chiller; energy saving; electric-load tracking

1. Introduction

Cogeneration (or CHP, Combined Heat and Power) represents a mature and well-known technology, able to ensure remarkable energy and economic savings, due to the combined production of thermal end electric energy, from a single primary energy input [1,2]. Trigeneration systems are CHP units whose thermal waste energy is also used to drive a thermally-driven chiller. Such systems are often referred to as Combined Cooling, Heat and Power (CCHP) systems [3]. CCHP systems can be also used to produce other products (e.g., hydrogen, alcohols, glycerine), configuring a polygeneration system [4].

CHP and CCHP are based on the recovery of the exhaust heat rejected by an engine, also called the prime mover (PM) [5]. Such thermal energy may be used for heating, process, production of sanitary hot water, etc., and/or to drive a thermally-driven chiller to produce cooling energy [1,6]. The main

advantages of CHP/CCHP systems are: (i) energy and economic savings and reduction of greenhouse gas emissions with respect to the separate production of the same amounts of energy with conventional technologies [1]; (ii) higher flexibility in power dispatch [5]; (iii) scalability [5]; (iv) energy reliability [5].

CCHP/CHP systems exhibit good economic, energy and environmental performance for a large number of applications, such as: large-sized industries [7]; chemical industries [8]; hospitals [9]; food industries [10], paper mills [11].

The literature is rich of papers dealing with cogeneration, also investigating several aspects of CHP/CCHP operating conditions [12] and control strategies [5].

Ref. [13] deals with a combined cycle CCHP supplying a university campus. The CCHP layout is based on two gas turbines, each with a rated power of 11 MWe. Moreover, a backpressure steam turbine is installed, providing additional 5.5 MWe of power. This study proves that CCHP systems are useful for reducing the primary energy consumption of the campus [13].

In Ref. [14], a 425 kWe trigeneration system, based on an internal combustion engine, is coupled with a 355.2 kWth single effect absorption chiller (ACH). The system, installed in a Brazilian University, is simulated using the software COGMCI, comparing two control strategies: full load mode and electrical load tracking mode.

The dynamic simulation model of a 65 kWe microturbine was developed in Ref. [15], using Matlab. The aim of this work is to describe in detail a microturbine performance, including transient effects. The validation of the proposed model was performed using real measured data, provided by the microturbine installed at the Savona Campus of the University of Genova (Italy).

A polygeneration system based on a combined cycle was analysed in Ref. [16]. The waste heat of the combined cycle is exploited to generate steam and hot water, delivered to a hospital. The developed plant consists of a 46.6 MWe gas turbine and a 28.6 MWe steam turbine. A simulation model in ASPEN PLUS is developed to select the most profitable operating strategy [16]. An optimization tool was adopted in Ref. [17], aiming to define the best layout and operating strategy of a trigeneration plant supplying a hotel. Measured data were employed to model the energy demand of the building. In particular, this paper considers three system layouts: (i) reciprocating engine and single stage ACH; (ii) reciprocating engine and double stage ACH; (iii) gas turbine and double effect ACH. Several sensitive analyses were performed, also analysing the effects of a moderate tax exemption and those of a reduction of the fuel cost on the economic profitability of the systems [18].

In conclusion, many works are available in literature dealing with cogeneration/trigeneration technologies and applications, but only few papers implement a thermoeconomic analysis based on dynamic simulations, aiming to determine the optimal design and operating strategy of the system under evaluation. Such approach is adopted in the present paper, analysing a real case, represented by the CCHP system to be installed in a hospital located in Puglia, South Italy.

The system was designed by an ESCO (Energy Service COmpany), in the framework of an Energy Performance Contract, using a conventional engineering approach, based on standard steady state algorithms. The system was designed to cover a part of the thermal, cooling and power load of the complex. Conventional auxiliary systems are used to match the hospital demand when the CCHP unit is off and/or when its capacity is lower than the demand, namely electric chillers for cooling, condensing boilers for heating and public grid for power.

Since the system under analysis is an existing one, the simulation model was not used to investigate its optimal design, but rather to analyse its energy and economic performance in detail and to evaluate its optimal operating strategy. All design data used in the analysis correspond to the equipment selected by the ESCO for installation.

2. Plant Layout

In Figure 1, the layout of the CCHP system under consideration is represented. The system is based on a natural gas-fueled internal combustion engine, coupled with a single effect LiBr-H_2O absorption chiller. The trigeneration system, in an exercise from December 2019, was integrated into

the existing heating and cooling systems, which are still used as back-up and auxiliary systems; the system operates in parallel with the external public grid, to match the power demand when the engine is off and/or its capacity is not sufficient to this scope. The demand for thermal energy includes the production of sanitary hot water, steam, space heating and cooling. The electric energy is used for lights, machinery, medical devices, pumps, fans. An electrical load tracking mode was selected by the company who manage the system, and the maximum electric power of the CHP system is lower than the maximum power demand, in order to reduce the capital cost of the system and the running time in part load conditions. Therefore, when the power demand is lower than the cogenerator maximum capacity, such demand is fully supplied by the CHP unit; in other cases, the cogeneration unit operates at full load and a certain amount of power must be imported from the public grid. As a consequence, the availability of waste heat for heating and/or cooling purposes varies, according to the operating conditions of the engine. At any rate, the heat demand is usually much higher than the capacity of the CHP system, so that the auxiliary heaters are always active, and the same happens for the cooling demand.

The heat recovery system includes various loops, as described in the following. In the Exhaust Gases Loop (EGL), the Exhaust Gases (EG) leaving the engine (at a temperature of about 411 °C) are used to produce steam in the Steam–Exhaust Gas heat exchanger (S–EG-HE), evolving within the Steam Loop (SL); afterwards, in the EG-JW-HE, the exhaust gases are used to enhance the temperature of the engine jacket water (JW), flowing within the JW Loop (JWL), and finally leave the heat exchange section at a temperature of at least 120 °C (to avoid acid condensation phenomena inside the heat exchangers).

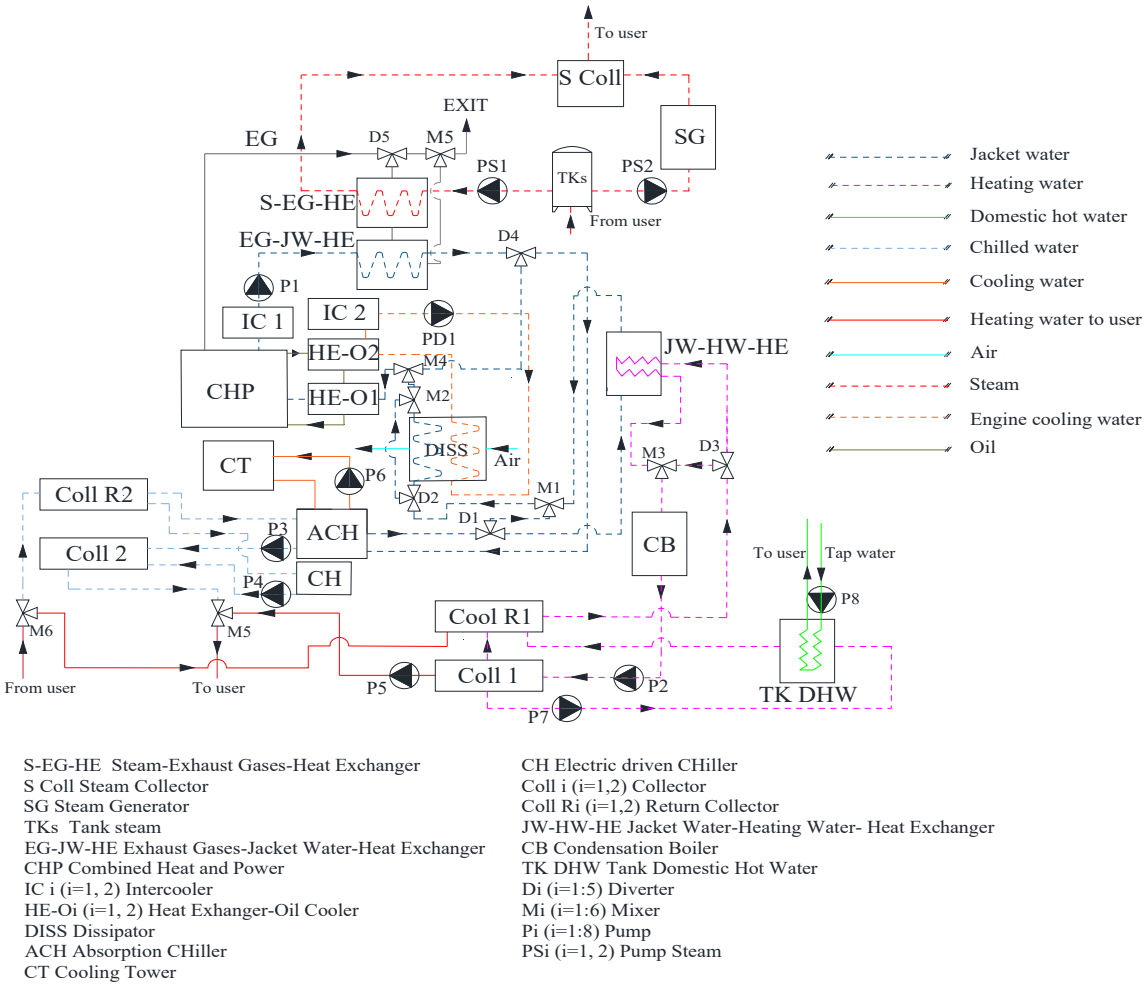

S-EG-HE Steam-Exhaust Gases-Heat Exchanger
S Coll Steam Collector
SG Steam Generator
TKs Tank steam
EG-JW-HE Exhaust Gases-Jacket Water-Heat Exchanger
CHP Combined Heat and Power
IC i (i=1, 2) Intercooler
HE-Oi (i=1, 2) Heat Exhanger-Oil Cooler
DISS Dissipator
ACH Absorption CHiller
CT Cooling Tower
CH Electric driven CHiller
Coll i (i=1,2) Collector
Coll Ri (i=1,2) Return Collector
JW-HW-HE Jacket Water-Heating Water- Heat Exchanger
CB Condensation Boiler
TK DHW Tank Domestic Hot Water
Di (i=1:5) Diverter
Mi (i=1:6) Mixer
Pi (i=1:8) Pump
PSi (i=1, 2) Pump Steam

Figure 1. Layout of the Combined Cooling, Heat and Power (CCHP) system under analysis.

As described in Figure 2, if the vapor produced in S–EG-HE ($Q_{steam,S\text{-}EG\text{-}HE}$) is lower than the hospital demand (Q_{steam}), the remaining amount of steam is produced by the auxiliary steam generator (SG). In particular, to this end, a suitable amount of water is sent from TKs to SG, by means of the pump PS2. The steam flows produced by S–EG-HE and/or SG are mixed in the steam collector (SColl), and finally are made available to the end users.

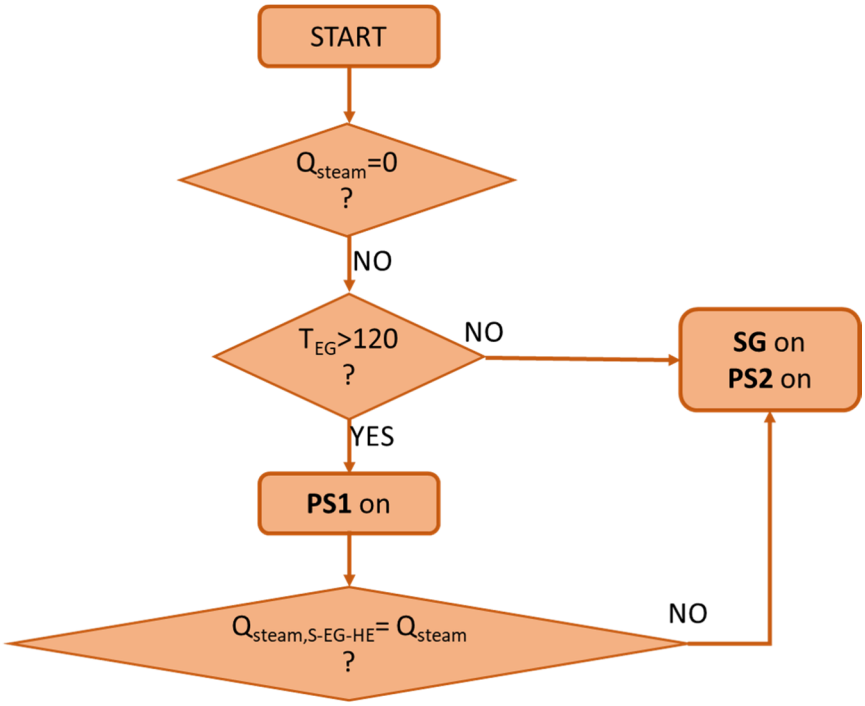

Figure 2. Steam Loop control strategy.

For the JW Loop, two different operation strategies are adopted, for heating and cooling periods, respectively. During the cooling period, the jacket water is primarily supplied to the absorption chiller (ACH), as shown in Figure 3; subsequently, the JW leaving the ACH is supplied to the JW-HW-HE (Figure 1) to provide heat to the heating water Loop. As shown in Figure 4, if the jacket water temperature decreases below 80 °C, the diverter D4 addresses the flow to the mixer M4, keeping the JW temperature within the range suggested by the engine manufacturer [19]. Conversely, if temperature of the jacket water rises over 80 °C, the dissipator unit is activated, preventing engine overheating. Clearly, if the cooling energy demand is null, the JW directly heats the heating Loop through the HE-H. Finally, JW cools down the engine oil in the HE-O1 exchanger.

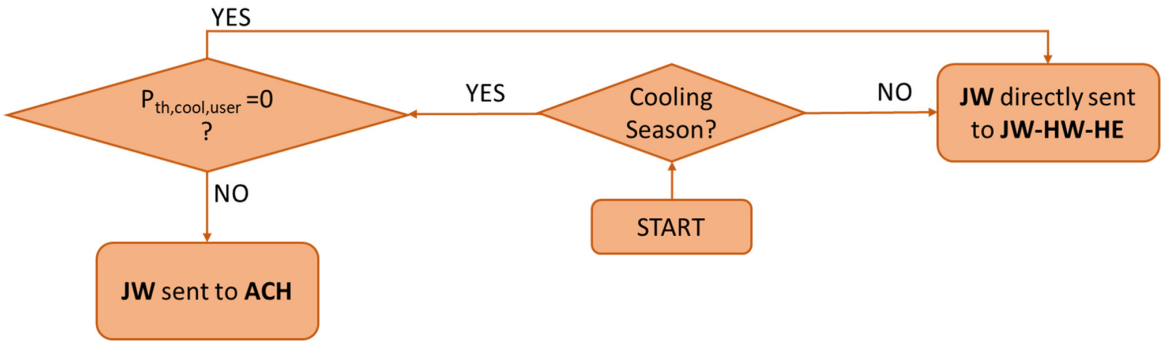

Figure 3. Control strategy regarding absorption chiller (ACH) and JW-HW-HE (Figure 1).

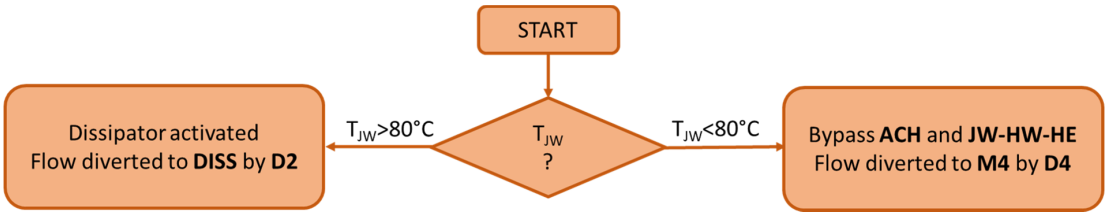

Figure 4. Control strategy of Jacket Water Loop.

The engine lubricating oil, flowing in the Oil Loop (OL), is cooled in HE-O1, supplying heat to jacket water, and in and HE-O2, where low temperature heat is dissipated in the heat exchanger DISS.

The Engine Water Cooling Loop (EWCL) is used to cool the second stage of intercooling (IC2) and the engine oil (HE-O2)—since the temperature within this loop is too low, the thermal energy of the loop is entirely dissipated in the dissipator (DISS).

The heating water Loop (HWL) consists of the water heated in JW-HW-HE, which supplies thermal energy for building space heating and domestic hot water (DHW). In particular, in JW-HW-HE the heat exchange between JW and heating water (HW) is performed, increasing the temperature of HW. Subsequently, HW is supplied to the heating water collector (Coll 1). Note that the setpoint temperature of HWL is 85 °C. If the temperature of HWL is below 85 °C, the auxiliary condensation boiler (CB) is activated, raising such temperature to 85 °C (Figure 5). The HWL is managed by pump P2, which is turned on only when there is a demand for space heating and/or the top temperature of the domestic hot water tank ($T_{top,TKDHW}$) decreases below 45 °C (Figure 6). In particular, when $T_{top,TKDHW}$ decreases below 45 °C, the pump P7 is also switched on, supplying thermal energy to TKDWH. The pump P7 is switched off when $T_{top,TKDHW}$ reaches the value of 60 °C.

The Domestic Hot Water Loop (DHWL) refers to the sanitary hot water required by the hospital. When the DHW demand is not null, the pump P8 is switched on. Thus, a proper amount of water flows through the heat exchanger towards the tank TKDHW, heating the water from 15 °C (tap water) to 45 °C.

The Building space Heating loop (BHL) refers to the hot water supplied to the fain-coils inside the hospital. In the heating period, the pump P5 is switched on, keeping the indoor temperature equal to the its setpoint value (Table 2).

The Building space Cooling Loop (BCL) is used to provide space cooling by means of Chilled Water (CW), supplied to fan coils located in the building. The cooling demand is matched by the ACH, as far as possible; when the ACH capacity is not sufficient, the auxiliary electric chillers (CH) are activated.

The Cooling Tower Water Loop (CTWL) is used to cool all the chillers included in the plant (ACH and CH); therefore, when ACH and/or CH are running, the pump P4 must be activated.

As mentioned before, an electric load tracking operating strategy was adopted for the system under evaluation. The engine can work with a partial load ratio (R_{el}, defined as the ratio of the power demand on the maximum rated power) ranging between 50% and 100%; when R_{el} falls below 50%, the engine must be switched off.

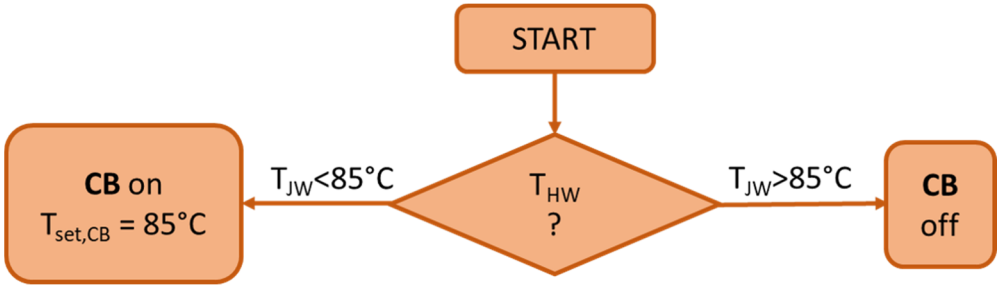

Figure 5. Hot Water Loop control strategy.

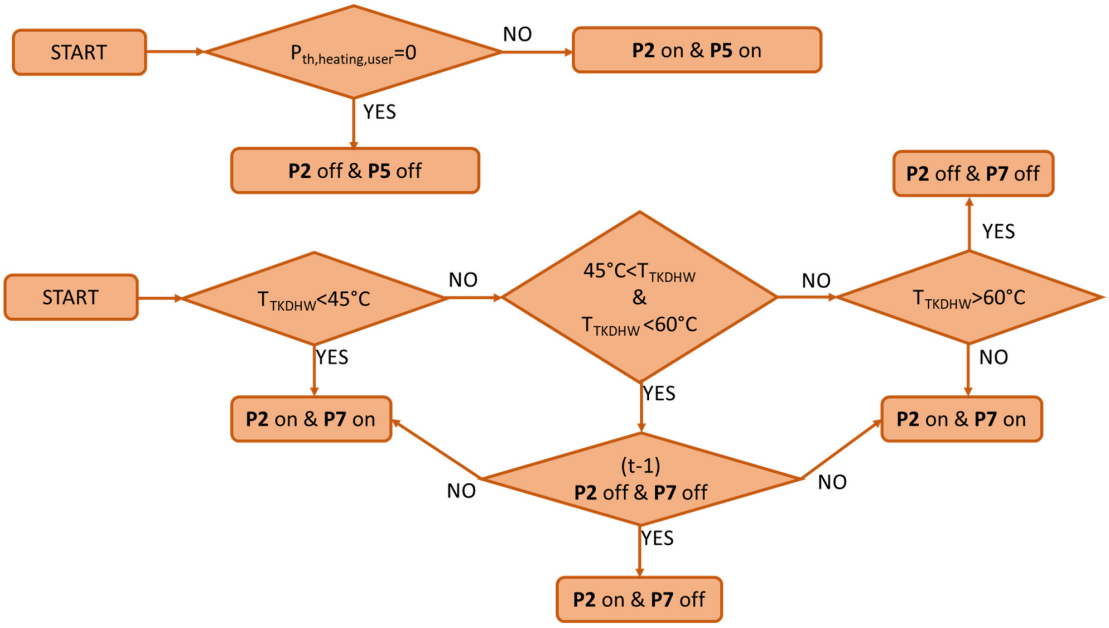

Figure 6. Control strategy regarding building space heating and Domestic Hot Water (DHW).

3. Simulation Model

The system presented was modelled in TRNSYS 17 environment. TRNSYS is widely employed in the academic community, because of its high accuracy and reliability; moreover, a large library of user-developed models and experimentally validated built-in components [20] is included in this software. The model includes several components (engine, heat exchangers, tanks, pumps, etc). Some of these models are based on thermodynamic models and they are mainly taken from TRNSYS library, being previously validated against experimental data and successfully used in several works. The Type 56 (Building) is considered a reference in the field of building dynamic simulation. The 3D geometric model of the hospital was built with the Google SketchUp TRNSYS 3d plug-in; such geometric model was then imported in the Type 56.

The main TRNSYS libraries used in this work are described below.

- Type 56: this library dynamically models the energy performance of the building considering its 3D geometry, thermophysical proprieties of the envelope, dynamic weather conditions (i.e., solar radiation, ambient temperature, wind velocity, relative humidity, etc.); further details are available in Ref. [21].
- Type 907: this library describes the performance of internal combustion engines, considering oil cooling water, after-cooling water, jacket water, and using inlet air temperature as a parameter. The mass and thermal balance performed by this library are based on manufactured data [18]. For the sake of brevity, the equations of this model not are described here, but a detailed description is available in Ref. [1].
- Type 107: this library models the performance of a single-effect LiBr-H_2O absorption chiller. The library adopts a normalized catalogue data look-up principle [22]. Thus, the performance of ACH is evaluated by using an operating map provided by manufacturers [23]. Further details are reported in Ref. [1].

3.1. Energy Analysis

A comparison between the Proposed System (*PS*) described above and a conventional, Reference System (*RS*) was carried out. The energy comparison was performed by evaluating the Primary Energy consumptions (*PE*) of both *RS* and *PS*, and the corresponding Primary Energy Saving (*PES*) achieved by the *PS*. In particular, *PE* and *PES* were calculated as follows:

$$\begin{aligned} PE_{RS} &= \left[\frac{\left(E_{el,LOAD}+\frac{E_{th,cool}}{COP}\right)}{\eta_{el}} + \frac{\left(E_{th,heat}+E_{th,DHW}\right)}{\eta_{CB}} + \frac{E_{th,vapor}}{\eta_{SG}}\right]_t \\ PE_{PS} &= \sum_t \left[PE_{CHP} + \frac{E_{el,fromGRID}}{\eta_{el}} + \frac{E_{th,auxCB}}{\eta_{CB}} + \frac{E_{th,auxSG}}{\eta_{SG}}\right]_t \\ PES_{PS} &= \frac{PE_{RS}-PE_{PS}}{PE_{RS}} \end{aligned} \quad (1)$$

Here, $E_{el,load}$ is the overall electric energy demand of the hospital, $E_{th,cool}$ and $E_{th,heat}$ are the thermal energy demand for space cooling and heating, respectively, $E_{th,DHW}$ is the thermal energy demand for sanitary hot water production, $E_{th,steam}$ is the thermal energy needed for steam production, $E_{el,fromGRID}$ is the electric energy withdrawn from the grid, $E_{th,CB}$ and $E_{th,SG}$ are the thermal energy provided by auxiliary boilers and steam generators, respectively; the remaining terms in Equation (1) are explained in Table 1.

3.2. Economic Analysis

The yearly operating cost (*C*) of *RS* and *PS* are calculated as follows:

$$\begin{aligned} C_{RS} &= \left[J_{el,fromGRID}\left(E_{el,LOAD} + \frac{E_{th,cool}}{COP}\right) + J_{NG}\frac{\left(E_{th,heat}+E_{th,DHW}\right)}{\eta_{CB}} + J_{NG}\frac{E_{th,vapor}}{\eta_{SG}}\right]_t \\ C_{PS} &= \left(\frac{E_{th,auxCB}}{\eta_{CB}} + \frac{E_{th,auxSG}}{\eta_{SG}}\right)J_{NG} + C_{CHP} + E_{el,fromGRID}J_{el,fromGRID} - J_{ESC}ESC + M_{CHP} \\ C_{CHP} &= V_{CHP}LHV_{NG}J_{NG,CHP} \end{aligned} \quad (2)$$

Table 1 explains the main terms of these equations. The subsidies available in Italy for cogeneration (Energy Saving Certificates, ESC) were considered; they are proportional to the primary energy saving acknowledged as "*High-Efficiency cogeneration*" units, and can be calculated with an algorithm described in Ref. [1].

Table 1. Thermoeconomic and environmental assumptions.

Parameter	Description	Value	Unit
$J_{el,fromGRID}$	Grid electric energy unit cost	180	€/MWh
J_{NG}	Average Natural gas unit cost for boilers and steam generators	29.5	€/MWh$_{PE}$
$J_{NG,CHP}$	Average Natural gas unit cost for CHP	27.5	€/MWh$_{PE}$
J_{ESC}	Economic value of ESC	180	€/ESC
LHV_{NG}	Natural gas lower heating value	9.59	kWh/Sm^3
η_{el}	Conventional thermo-electric power plant efficiency	46	%
η_{CB}	Natural gas condensing boiler efficiency	95	%
η_{SG}	Natural gas steam generator efficiency	75	%
AF	Annuity factor	8	years

The economic performance of the proposed system was evaluated by means of the following economic parameters: (i) yearly economic savings (ΔC); (ii) Simple payback period (*SPB*) of the investment; (iii) net present value (*NPV*); and (iv) profitability index (*PI*):

$$\begin{aligned} \Delta C &= \frac{C_{RS}-C_{PS}}{C_{RS}} \\ SPB &= \frac{C_{inv}}{\Delta C} \\ PI_{PS} &= \frac{\Delta C \cdot AF - C_{inv}}{C_{inv}} \\ NPV &= PIC_{inv} \end{aligned} \quad (3)$$

Here, C_{inv} is the capital cost of the cogeneration plant, equal to 2.0 M€, and AF is the annuity factor, assumed equal to eight years (based on a discount rate of 5% and a time horizon of 10 years—Table 1).

4. Hospital Energy Loads

The system described above is to be installed in the "F. Miulli" hospital, located in Acquaviva delle Fonti, near Bari, in South Italy (Figures 7 and 8). The facility has 603 beds and a gross volume of 370×10^3 m^3.

To limit the computational cost of the simulations, while keeping the accuracy high, the complex of buildings was thermally modelled by defining four thermal zones (Table 2 and Figure 7), characterized by similar features and destination (Figure 7): Zone A includes the operating rooms, Zone B the resting rooms, Zone C offices and clinic rooms, Zone D technical rooms.

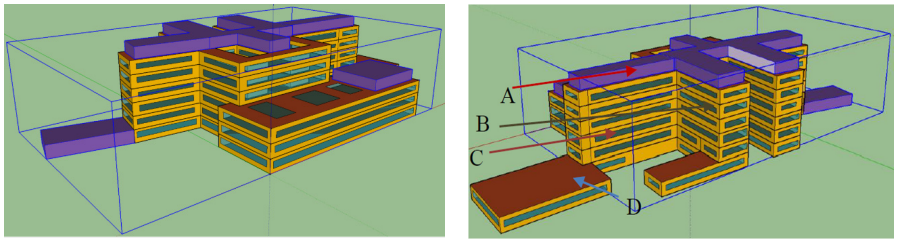

Figure 7. Building model, front side (**left**), back side (**right**).

The occupancy schedule of such thermal zones is reported in Table 2. Here, data about the main geometric characteristics, ventilation, setpoint temperatures and heating and cooling periods for each thermal zone are reported, too. The elements of the building envelope are described in Table 3. Note that, as it is well-known, the thickness and U-value of each element affect the energy performance of the building in terms of space heating and cooling energy consumption. The hospital is located in the Italian weather zone D (1.610 heating degree-day, Table 2). It is useful to remember that the heating degree-days of a site are defined as the sum of the difference (considered only if positive) between the indoor setpoint temperature and the mean daily outdoor temperature of that site. In the heating season, such parameter is commonly used to estimate the energy consumption for space heating of buildings.

According to the Italian legislation about healthcare facilities, no restrictions are present concerning the duration of the heating periods.

Presently, the energy needs of the facility are matched as follows: electric air-to-air chillers, natural gas-fueled steam generators, for steam, and condensing boilers for sanitary hot water preparation and space heating; electric energy and natural gas; this configuration was adopted as the Reference System for the energy and economic analyses of the new CCHP system presented in the next section.

The hospital consumes about 15.89 GWh/y of electric energy and 1.76×10^6 Sm^3 of natural gas. Figure 9 shows the current electric energy and natural gas consumptions on a monthly basis.

In particular, three 3 MW TRANE CVGF1000 electric chillers combined with four 3.5 MW cooling towers are included for the production of chilled water; one chiller is used as a backup system. The power absorbed by each chiller is equal to equal to 504 kW. The total electric consumption of chillers and cooling towers is estimated at around 2909 MWh/year.

The Heating, Ventilation and Air Conditioning (HVAC) systems are responsible for the consumption of about 27 GWh/year, equal to 52% the total consumption. The 25 circulation pumps (including the spare ones) have a consumption of about 1566 MWh/year. The overall lighting consumption is equal to 8490 MWh/year (16% of the total consumption). A total of 37 lifts, covering six floors, consume around 350 MWh/year (1.5% of the total consumption). The two natural gas steam generators (model 2.1 MW HOVAL HG-E-240) consume about 1,080,000 Sm^3/year. The thermal energy demand for space heating and domestic hot water is covered by three natural gas boilers (model 3.5 MW HOVAL MAX-3), with a consumption of 685,000 Sm^3/year and 160,000 Sm^3/year, for heating and DHW, respectively.

Figure 8. Miulli hospital.

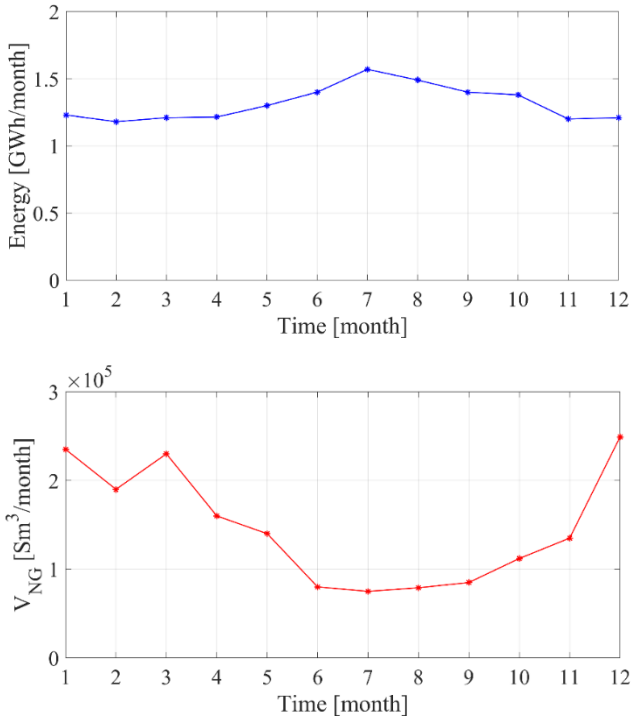

Figure 9. Electric energy and Natural gas monthly demand.

Table 2. Thermal zone simulation data.

-	A	B	C	D
Geometric Features: Volume (m^3)	9249.81	41624.2	44,787.2	19,655.9
Ventilation (vol/h)	15	3	3	1
$T_{set,winter}$(°C) $T_{set,summer}$(°C)	20 ± 1 23 ± 1	22 ± 2 24 ± 2	21 ± 1 26 ± 1	19 ± 1 26 ± 1
DHW set point temperature (°C)	45			
Heating and cooling season (1.610-degree day)	15th November–31st March 1st May–30th September			
Occupancy schedule	00:00–24:00	00:00–24:00	08:00–18:00	00:00–24:00
Simulation Time step (h)	0.05			

Table 3. Elements of the building envelope.

Building Element	Zones A & B & C & D			
	U-Value (W/m^{2}K)	Thickness (m)	ρ_s (–)	ε (–)
Roof	0.600	0.235	0.4	0.9
Façades	0.492	0.280		
Ground floor	0.608	0.560		
Adjacent ceiling	1.111	0.400		
Windows glass	2.89	0.004/0.016/0.004	0.13	0.18

The layout of the cogeneration system to be installed was already presented in Figure 1. The CHP unit is an internal combustion engine model *ABB Ecomax 20*, with a rated power of 2.00 MW and a thermal capacity of 1.95 MW [18] (Table 4); the nominal electric efficiency is 44.1%, the thermal one 43.0%; therefore, the global efficiency is equal to 87.1%.

Table 4. Design and operating parameters.

Component	Parameter	Value	Unit
CHP system	Model	Ecomax 20 HE	
	Manufacturer	AB	
	Rated thermal capacity	1882	kW
	Rated electrical capacity	2004	
	Rated fuel input	4544	
	Rated electrical efficiency	44.1	%
	Rated thermal efficiency	43.0	
	Global rated efficiency	87.1	
Heat exchanger exhaust gas-condensed vapor	Rated thermal capacity	750	kW
	Condensed water flow rate	1284	kg/h
	Exhaust gas flow rate	10,753	
Dissipator (DISS)	Rated thermal capacity	1300	kW
DHW heat exchanger (DHWHE)	Efficiency	50	%
	Average DHW flow rate demand (P8)	1360	kg/h
	Heating water flow rate (P7)	40,480	
Auxiliary boiler (heating loop CB)	Rated thermal capacity	10,500	kW_{th}
Auxiliary boiler (vapor loop CBVap)	Rated thermal capacity	4000	kW_{th}
Electrical auxiliary chiller	Rated thermal capacity	9000	kW_{th}
	COP	5.95	-
Absorption chiller	Rated cooling capacity	769	kW
	Setpoint temperature for the chilled water	7	°C
Cooling tower	Rated thermal capacity	1794	kW

According to the indications provided by the ESCO, who designed the plant, an electric load tracking operating strategy was adopted. Table 4 also displays the characteristics of other devices included in the layout under analysis. Note that the existing devices, such as steam generators and condensing boilers, are employed as auxiliary systems, see Figure 1.

In conclusion, the case study presented above was solved in the TRNSYS environment, selecting an equation-resolution time step of 0.05 h, as shown in Table 2.

5. Results

In this section, the calibration of the building model is presented as well as the results of the simulations carried out are discussed. The calibration is performed using the data regarding the energy bills. In particular, for each month of the year, the comparison between the real data of thermal energy demand for space heating and domestic hot water and the simulated value by the implementation of the building model is presented (Figure 10). The same comparison is presented also for the total electric demand, including also the electric consumption to supply the electric chillers for the hospital space cooling. Figure 10 clearly shows a good agreement between the numerical results and real data. Therefore, the building model resulted to be calibrated.

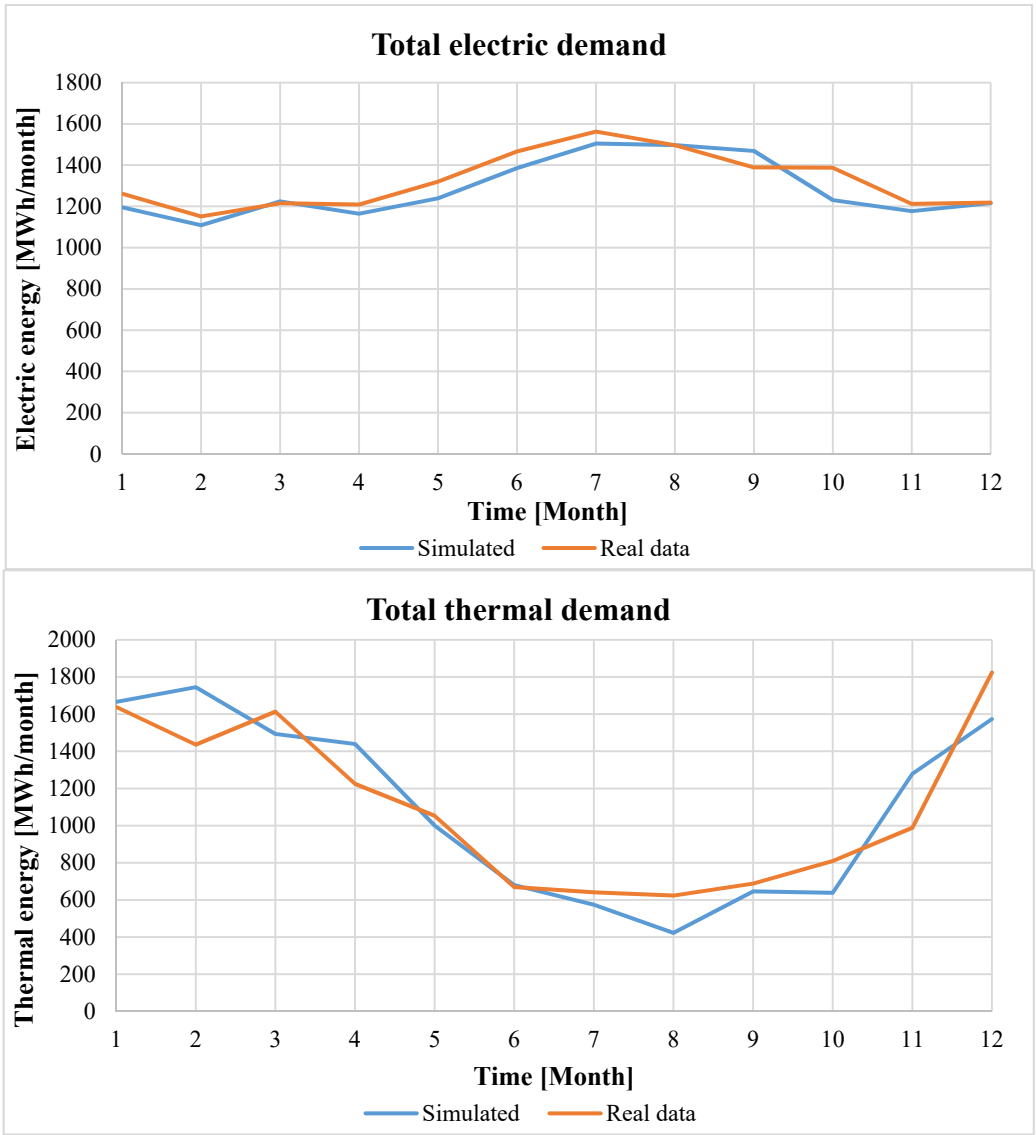

Figure 10. Calibration: thermal and electric energy demand of the hospital. Simulated data vs. real data.

5.1. Daily Results

Figure 11 displays the dynamic performance of the CCHP under evaluation. The power ($P_{el,CHP}$) varies over the hours, due to the control strategy assumed (electric load tracking). In particular, in the case shown in the figure, $P_{el,CHP}$ is constantly equal to the power demand of the hospital ($P_{el,LOAD}$). The latter, in fact, is never higher than the maximum power of the CCHP system. Moreover, Figure 11 displays the thermal control strategy adopted, aiming at keeping the jacket water temperature entering the engine ($T_{JW,inCHP}$) equal to about 80 °C.

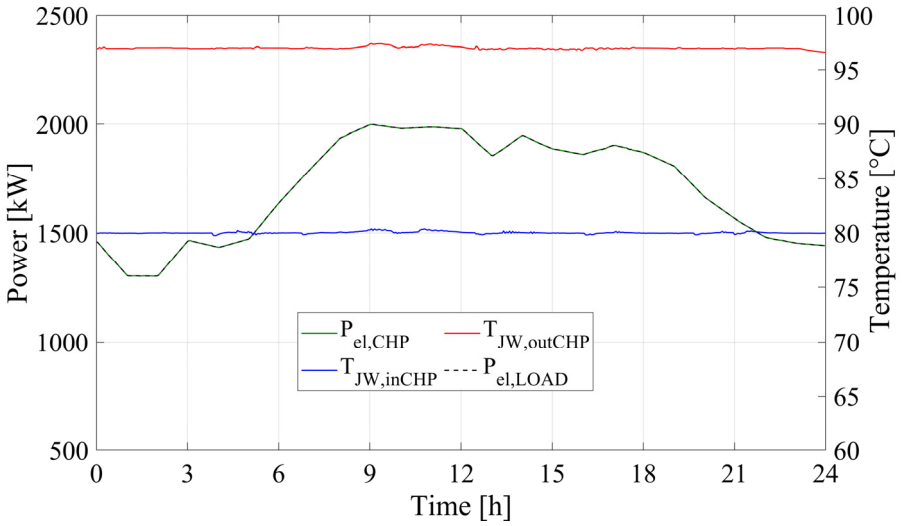

Figure 11. Dynamic performance of the cogeneration system—daily results.

5.2. Weekly Results

Figure 12 displays the weekly energy performance of the proposed layout. According to the operating strategy adopted for the system, it is able to constantly match the electric energy demand of the hospital (Figures 11 and 12—left side). Note that some weeks are characterized by zero or limited energy production, due to scheduled maintenance interventions. Clearly, when the engine is switched off, the public grid is used as a backup system, meeting the electric energy demand of the hospital. The electric energy delivered to the auxiliary systems is very low, achieving the maximum value of 10 MWh/week (Figure 12—left side). The thermal energy recovered by the engine ($E_{th,CHP}$) is equal to about 281-310 MWh_{th}/week (Figure 12—right side). In particular, the medium temperature thermal energy ($E_{th,CHP,MT}$) ranges between 281–310 MWh_{th}/week, whereas the high temperature one ($E_{th,CHP,HT}$) ranges between 109 and 129 MWh_{th}/week (Figure 12—right side).

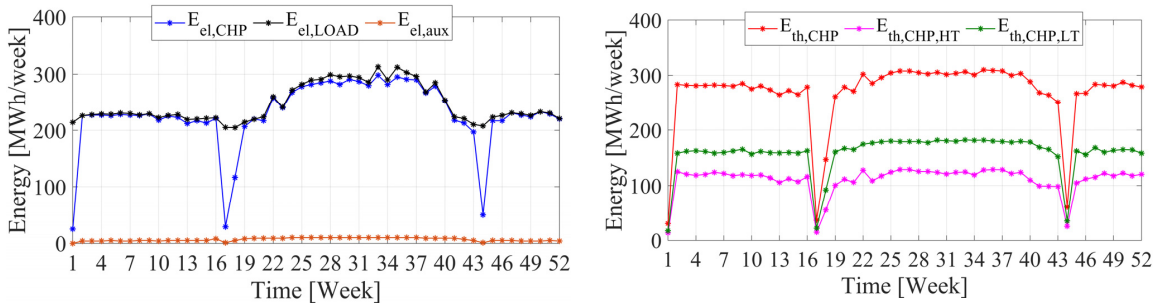

Figure 12. Energy performance of the proposed layout: electric energy (**left**) and thermal energy (**right**).

Figure 13 displays the performance of the Steam Loop (SL), and, in particular, the thermal energy required for steam production ($E_{th,Steam}$), and the ratio of the thermal energy provided by the steam generator (SG) and by the CHP system to the overall request, $E_{th,Steam}$ (R_{SG} and $R_{CGP,HT}$, respectively). From Week 28 to week 35 (summer period), the thermal energy provided by SG for producing steam is about null, i.e., R_{SG} is equal to zero. This trend is due to the reduction of the demand of steam during these weeks. During the remaining weeks, the CHP system is able to meet a limited share of $E_{th,Steam}$: $R_{CGP,HT}$ ranges between 42% and 57%, except the weeks in which the programmed maintenance operations occur (weeks 17 and 44).

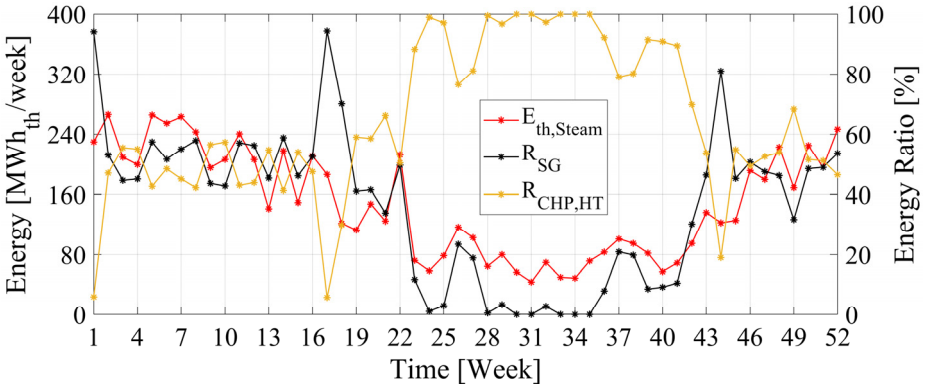

Figure 13. Energy performance of the Proposed System—Steam production.

Figure 14 displays the weekly energy balance regarding the cooling service; in particular, the following quantities are shown: cooling energy demand ($E_{th,cool}$), ratio of the cooling energy provided by ACH on $E_{th,cool}$ (R_{ACH}), and ratio of cooling energy provided by the electric-driven auxiliary chiller on $E_{th,cool}$ (R_{CH}). When the cooling demand is high (weeks from 25 to 36), the ACH is able to match the major share of cooling energy demand (R_{CH} ranging from 56% to 76%).

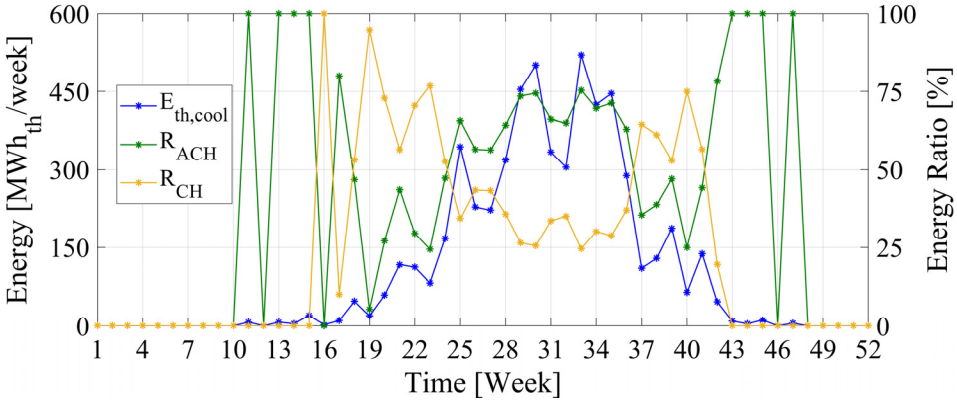

Figure 14. Energy performance of the Proposed System—Cooling demand.

5.3. Yearly Results

Table 5 summarizes the yearly performance of the proposed layout. CHP produces 13.74 GWh/year of electric energy, achieving an electric efficiency of 42%. The proposed system exhibits a limited energy saving (*PES* equal to 9%). This is mainly due to the fact that the energy saving was calculated with respect to the overall primary energy consumption of the reference scenario, whereas the Proposed System only covers a part of such consumption. in particular, the share of thermal energy produced by the CHP on the overall request is only 41% (Table 6). Should the energy saving be calculated for the cogeneration system only, it would be significantly higher.

In any case, from the economical point of view, the Proposed System achieves significant results, with an SPB of 1.5 years and an *NPV* of 7.10 M€ (Table 5). The economic results are mainly due to two elements: first, the proposed CHP is able to achieve a remarkable amount of energy savings certificates (*ESC*), whose market value amounts to 0.207 M€/year; second, energy prices are considerably high in Italy, therefore self-production causes significant economic savings. Therefore, even if the primary energy saving is moderate (about 9%), the economic profitability is excellent.

Table 5. Yearly result summary.

$E_{th,CHP}$	$E_{el,CHP}$	ΔPE	PES	η_{el}	η_{th}	η	ESC	SPB	ΔC	PI	NPV
(GWh_{th}/year)	(GWh/year)	(GWh/year)	(%)				(M€/year)	(years)	(M€/year)	(-)	(M€)
13.19	13.74	3.27	8.9	42.1	39.42	72.54	0.207	1.5	1.22	3.88	7.10

Table 6. Share of energy demand covered by the CCHP system.

$E_{el,fromGRID}/E_{el,LOAD}$	$E_{el,CHP}/E_{el,LOAD}$	$E_{th,CHP,usefull}/E_{th,demand}$	$E_{th,ACH}/E_{th,cool}$
(%)			
7.9	92.1	40.65	28.00

6. Conclusions

The paper presents the energy and economic analysis of a trigeneration system, installed in a hospital located in South Italy. In this scope, a detailed dynamic simulation model was developed in TRNSYS, in order to analyse the behaviour of the proposed system, whereas real data were used about the energy consumption, people scheduling and thermophysical characteristics of the hospital.

The main results are summarized below:

- the trigeneration system produces about 13.74 GWh/year of electric energy with an electric efficiency of 42%; in particular, 92% of the electric energy demand of the hospital is met by the system;
- a limited share of the overall thermal energy demand of the hospital is matched by the cogeneration unit (41%); this is due to the fact that the size of the system was mainly selected on the basis of the power demand of the hospital (much lower than the thermal one), to avoid: (i) the production of excess electric energy (in case of full-load operation or thermal load tracking); (ii) the need for continuous part-load operation, in case of electric load tracking (this latter represents the option actually selected for the system under consideration);
- in spite of a limited primary energy savings index (about 9%), mainly due to the limited share of thermal energy covered by the cogeneration system, excellent economic performance was highlighted by the simulations (payback period equal to 1.5 years, profitability index of 3.88), also due to the significant contribution of the subsidies provided by the current Italian regulation for CHP systems (energy savings certificates, with a market value of 0.207 M€/years).

Further analyses will be carried out, aiming to investigate the influence of the design choices on the performance of the system and the opportunities for improving the efficiency of the trigeneration system, as well as that of the hospital, as a whole.

Author Contributions: All authors provide equality contribute. All authors have read and agreed to the published version of the manuscript.

Funding: This research received no external funding.

Conflicts of Interest: The authors declare no conflict of interest.

Nomenclature

E	energy (kWh/MWh/GWh)
ESC	energy savings certificates (-)
J	capital cost (€)
NPV	net present value (€) electric power (kW)
P	electric power (kW)
PE	primary energy per year (GWh/year)
PES	primary energy saving index (-)
PI	profitability index (-)
SPB	simple payback period (years)
T	temperature (°C)
U	overall heat transfer coefficient (W m^{-2} K^{-1})
V	volume of natural gas (Sm3)

Greek Symbols

Δ	difference (-)
η	efficiency (-)
ρ	density (kg m^{-3})
ρ_s	solar reflectance (-)

Subscripts

ACH	absorption chiller
CB	condensing boiler
CH	electric chiller
CHP	combined heat and power system
CCHP	combined cooling, heat and power system
cool	cooling
EHW	domestic hot water
el	electric
LOAD	the electric energy demand of the user
from GRID	electric energy withdrawn from the public grid
heat	heating
HT	the high temperature thermal energy
MT	the medium temperature thermal energy
NG	natural gas
PS	proposed system
RS	reference system
t	referred to a generic time step
th	thermal
SG	steam generator
Steam	steam

References

1. Calise, F.; Dentice d'Accadia, M.; Libertini, L.; Quiriti, E.; Vanoli, R.; Vicidomini, M. Optimal operating strategies of combined cooling, heating and power systems: A case study for an engine manufacturing facility. *Energy Convers. Manag.* **2017**, *149*, 1066–1084. [CrossRef]
2. Faramarzi, G.R.; Khodakarami, M.; Shabani, A.; Saen, R.F.; Azad, F. New network data envelopment analysis approaches: An application in measuring sustainable operation of combined cycle power plants. *J. Clean. Prod.* **2015**, *108*, 232–246. [CrossRef]
3. Jiang, J.; Gao, W.; Wei, X.; Li, Y.; Kuroki, S. Reliability and cost analysis of the redundant design of a combined cooling, heating and power (CCHP) system. *Energy Convers. Manag.* **2019**, *199*, 111988. [CrossRef]

4. Murugan, S.; Horák, B. Tri and polygeneration systems - A review. *Renew. Sustain. Energy Rev.* **2016**, *60*, 1032–1051. [CrossRef]
5. Al Moussawi, H.; Fardoun, F.; Louahlia-Gualous, H. Review of tri-generation technologies: Design evaluation, optimization, decision-making, and selection approach. *Energy Convers. Manag.* **2016**, *120*, 157–196. [CrossRef]
6. Chicco, G.; Mancarella, P. From cogeneration to trigeneration: Profitable alternatives in a competitive market. *Ieee Trans. Energy Convers.* **2006**, *21*, 265–272. [CrossRef]
7. Gonzales Palomino, R.; Nebra, S.A. The potential of natural gas use including cogeneration in large-sized industry and commercial sector in Peru. *Energy Policy* **2012**, *50*, 192–206. [CrossRef]
8. Szklo, A.S.; Soares, J.B.; Tolmasquim, M.c.T. Economic potential of natural gas-fired cogeneration—Analysis of Brazil's chemical industry. *Energy Policy* **2004**, *32*, 1415–1428. [CrossRef]
9. Gimelli, A.; Muccillo, M.; Sannino, R. Optimal design of modular cogeneration plants for hospital facilities and robustness evaluation of the results. *Energy Convers. Manag.* **2017**, *134*, 20–31. [CrossRef]
10. Bianco, V.; De Rosa, M.; Scarpa, F.; Tagliafico, L.A. Implementation of a cogeneration plant for a food processing facility. A case study. *Appl. Therm. Eng.* **2016**, *102*, 500–512. [CrossRef]
11. Shabbir, I.; Mirzaeian, M. Feasibility analysis of different cogeneration systems for a paper mill to improve its energy efficiency. *Int. J. Hydrog. Energy* **2016**, *41*, 16535–16548. [CrossRef]
12. Calise, F.; Dentice d'Accadia, M.; Libertini, L.; Quiriti, E.; Vicidomini, M. A novel tool for thermoeconomic analysis and optimization of trigeneration systems: A case study for a hospital building in Italy. *Energy* **2017**, *126*, 64–87. [CrossRef]
13. do Espirito Santo, D.B. An energy and exergy analysis of a high-efficiency engine trigeneration system for a hospital: A case study methodology based on annual energy demand profiles. *Energy Build.* **2014**, *76*, 185–198. [CrossRef]
14. Espirito Santo, D.B. Energy and exergy efficiency of a building internal combustion engine trigeneration system under two different operational strategies. *Energy Build.* **2012**, *53*, 28–38. [CrossRef]
15. Bracco, S.; Delfino, F. A mathematical model for the dynamic simulation of low size cogeneration gas turbines within smart microgrids. *Energy* **2017**, *119*, 710–723. [CrossRef]
16. Zheng, L.; Furimsky, E. ASPEN simulation of cogeneration plants. *Energy Convers. Manag.* **2003**, *44*, 1845–1851. [CrossRef]
17. Piacentino, A.; Gallea, R.; Cardona, F.; Lo Brano, V.; Ciulla, G.; Catrini, P. Optimization of trigeneration systems by Mathematical Programming: Influence of plant scheme and boundary conditions. *Energy Convers. Manag.* **2015**, *104*, 100–114. [CrossRef]
18. Available online: https://www.gruppoab.com/it/ (accessed on 12 January 2019).
19. Klein, S.A. *TRNSYS-A Transient System Simulation Program*; Engineering Experiment Station Report; University of Wisconsin-Madison: Madison, WI, USA, 1988; pp. 12–38.
20. Murray, M.C.; Finlayson, N.; Kummert, M.; Macbeth, J. Live Energy Trnsys—Trnsys Simulation within Google Sketchup. In Proceedings of the 475 Eleventh International IBPSA Conference, Glasgow, Scotland, 27–30 July 2009.
21. Buonomano, A.; Calise, F.; Palombo, A.; Vicidomini, M. BIPVT systems for residential applications: An energy and economic analysis for European climates. *Appl. Energy* **2016**, *184*, 1411–1431. [CrossRef]
22. Handbook, A. *HVAC Systems and Equipment*; American Society of Heating, Refrigerating, and Air Conditioning Engineers: Atlanta, GA, USA, 1996; pp. 1–10.
23. Available online: http://www.enea.it/it (accessed on 22 December 2019).